In vivo Neuropathology: Detecting site-specific changes in neuroinflammation following treatment with low doses of known neurotoxins.

**D.S. ATHREYA[1], S. KEDHARNATH[1], A. PHADKE[1], P.P. KULKARNI[1], C.F. FERRIS[1,2]

[1]Center for Translational Neuroimaging, Northeastern Univ, Boston, MA USA, [2]Dept Psychology and Pharmaceutical Sciences, Northeastern Univ, Boston, MA

Northeastern University
Center for Translational Neuro-imaging

PSTR202.16 / W25

Background

Twenty-five percent of small molecules in drug development for CNS indications fail in clinical trials due to complications with previously undetected neurotoxicity. Indeed, it is very infrequent that a drug is flagged for neurotoxic side effects in early drug discovery. The consequences are two-fold: 1) loss of time and money in bringing new drugs to market and, 2) the unwitting exposure of patients in clinical trials to the neurotoxic side effects of what otherwise could be a drug candidate that is effectively treating the problem. To address this issue, we developed an MRI protocol "*in vivo* neuropathology" to identify putative areas of neuroinflammation using diffusion weighted imaging and computational analysis.

Experimental Design

Female rats, five per group, were treated with either a single IP injection for trimethyltin chloride (7mg/kg), a gold standard for CNS toxicity; a single IP injection of MK-801 (0.5mg/kg), an NMDA antagonist; a single IP injection of kainic acid (10mg/kg), a glutamate agonist; or 7-days gavage for BIA 10-2474 (1mg/kg), a FAAH antagonist. After administration, the rats were returned to their home cage to be left undisturbed until imaged 3 and 7 post administration for trimethyltin and 7 days post administration for all other groups.

Summary

Trimethyltin affected many brain areas (A.) The sensorimotor cortices (yellow) and hippocampus (red) were particularly sensitive. BIA 10-2474 (B.) was limited to the thalamus (blue). MK-801 (C.) affected many areas including the thalamus (blue) and cerebellum (green). Kainic acid (not shown) had no significant effect of DWI measures at the dose of 10mg/kg. Postmortem histology confirmed site-specific microglia activation following trimethyltin exposure (data not shown). Histological validation of microgliosis for BIA 10-2474 and MK-801 is in progress.

Highlights

- "*In vivo* neuropathology" is an imaging protocol using DWI and measures of ADC combined with computational analysis using a 3D MRI rat atlas with 173 brain areas to identify putative sites of neuroinflammation and edema following exposure to potential toxins.
- This non-invasive imaging protocol allows studies on time-dependent neuropathology.
- The global maps of neurotoxic injury can be used to guide histopathology during preclinical drug development.
- Analysis is achieved with a minimum number of rats adhering to the laws and regulations around the humane care and use of laboratory animals, providing an alternative to the traditional tests for assessing drug neurotoxicity.
- "*In vivo* neuropathology" can minimize the cost of preclinical CNS toxicology, expedite the process, and identify subtle changes in site-specific brain microarchitecture across the entire brain.

Results

Apparent Diffusion Coefficient: Vasogenic Edema

A. Trimethyltin

Trimethyltin	Pre TMT			Post TMT		
Brain Area	Ave	SD		Ave	SD	P val
crus 1 of ansiform lobule	2.16	0.39	>	1.62	0.10	0.020
lateral dorsal thalamus	2.24	0.26	>	1.80	0.13	0.020
medial septum	2.17	0.17	>	1.83	0.10	0.020
superior colliculus	2.63	0.16	>	2.03	0.19	0.020
visual 1 ctx	2.33	0.23	>	1.97	0.12	0.020
6th cerebellar lobule	2.44	0.24	>	1.90	0.19	0.021
CA1 dorsal	2.31	0.16	>	1.88	0.17	0.021
CA3 dorsal	2.32	0.23	>	1.87	0.13	0.021
anterior cingulate ctx	2.41	0.25	>	1.94	0.11	0.021
crus 2 of ansiform lobule	2.08	0.31	>	1.52	0.21	0.021
dentate gyrus dorsal	2.40	0.20	>	1.94	0.10	0.021
external plexiform layer	2.26	0.11	>	2.04	0.06	0.021
granular cell layer	2.19	0.11	>	1.91	0.04	0.021
lateral geniculate	2.22	0.23	>	1.81	0.10	0.021
lateral posterior thalamus	2.51	0.10	>	1.97	0.08	0.021
primary motor ctx	2.37	0.19	>	1.90	0.03	0.021
periaqueductal gray	2.56	0.27	>	2.06	0.12	0.021
parabrachial n.	2.45	0.38	>	1.90	0.16	0.021
parietal ctx	2.43	0.08	>	1.99	0.20	0.021
raphe obscurus n.	2.66	0.27	>	2.19	0.18	0.021
retrosplenial caudal ctx	2.54	0.16	>	2.27	0.04	0.021
retrosplenial rostral ctx	2.62	0.31	>	2.14	0.16	0.021
primary SS ctx forelimb	2.24	0.15	>	1.84	0.09	0.021
primary SS ctx hindlimb	2.49	0.30	>	1.91	0.14	0.021
primary SS ctx trunk	2.45	0.13	>	1.97	0.19	0.021
simple lobule cerebellum	2.47	0.28	>	1.84	0.19	0.021
visual 2 ctx	2.25	0.18	>	1.93	0.21	0.021
prelimbic ctx	2.02	0.14	>	1.77	0.09	0.029
primary SS ctx barrel field	2.20	0.12	>	1.86	0.13	0.029
central gray	2.70	0.34	>	2.13	0.16	0.042
7th cerebellar lobule	2.26	0.38	>	1.65	0.37	0.043
anterior pretectal n.	2.23	0.23	>	1.84	0.27	0.043
CA2	2.20	0.20	>	1.88	0.20	0.043
CA3 hippocampus ventral	2.29	0.21	>	2.02	0.14	0.043
dorsomedial tegmental area	2.32	0.33	>	1.88	0.19	0.043
flocculus cerebellum	2.49	0.37	>	2.00	0.19	0.043
inferior colliculus	2.73	0.26	>	2.21	0.28	0.043
lateral amygdaloid n.	2.35	0.21	>	1.99	0.21	0.043
locus ceruleus	2.86	0.46	>	2.06	0.18	0.043
medial geniculate	2.25	0.37	>	1.82	0.15	0.043
paraflocculus cerebellum	2.32	0.27	>	1.92	0.13	0.043
reticular n. midbrain	2.36	0.32	>	1.88	0.16	0.043
primary SS ctx jaw	1.98	0.08	>	1.77	0.14	0.043
primary SS ctx shoulder	2.36	0.25	>	1.93	0.16	0.043
secondary somatosensory ctx	2.00	0.19	>	1.69	0.14	0.043

B. BIA 10-2472

BIA 10-2474	Vehicle			BIA 10-2474		
Brain Area	Ave	SD		Ave	SD	P val
dorsal raphe	2.06	0.18	<	2.74	0.41	0.014
lateral geniculate thalamus	1.78	0.16	<	2.15	0.35	0.027
medial dorsal thalamus	1.81	0.16	<	2.16	0.27	0.027
supramammillary n.	2.19	0.38	<	2.95	0.44	0.037
ventral posteriolmedial thalamus	1.75	0.12	<	2.07	0.30	0.037
ventrolateral thalamus	1.76	0.14	<	2.06	0.28	0.049
anterior thalamus	1.84	0.16	<	2.11	0.26	0.050
habenula n. thalamus	2.27	0.33	<	2.84	0.34	0.050
reticular n. thalamus	1.86	0.12	<	2.14	0.28	0.050
ventral posteriolateral thalamus	1.77	0.14	<	2.06	0.29	0.050

Statistical Heat Maps: 2D Reconstructions

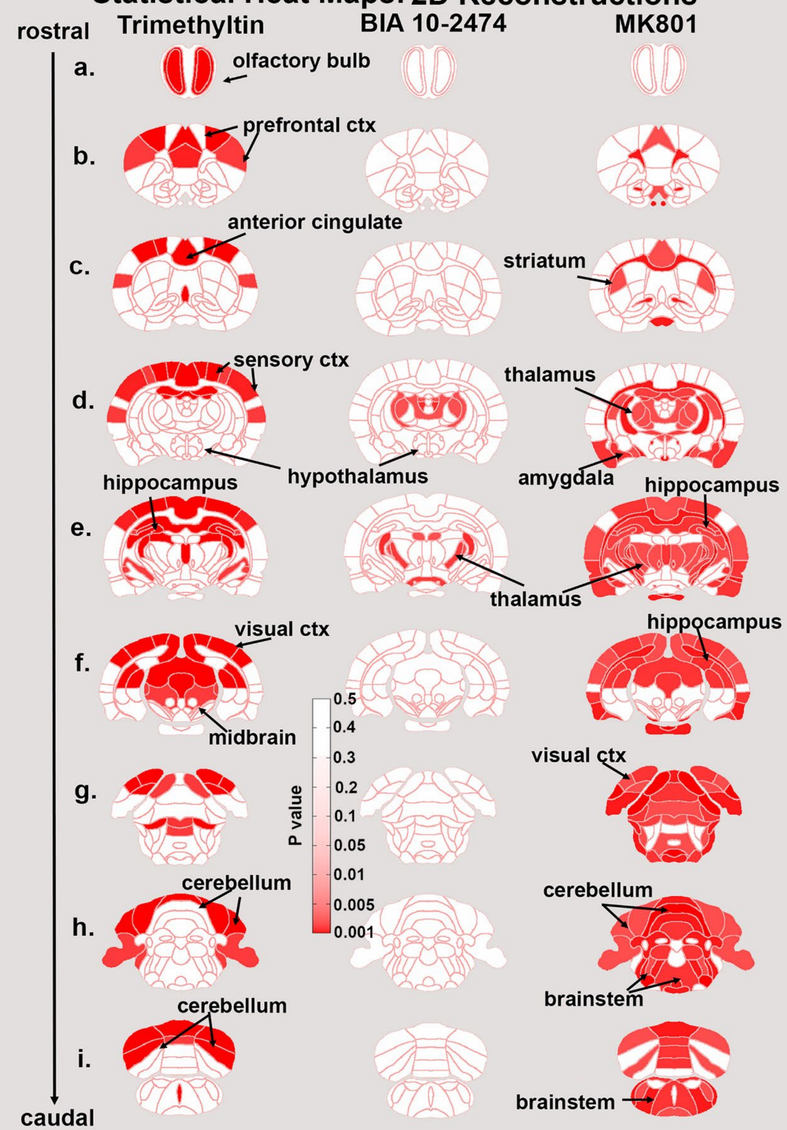

3D Reconstructions

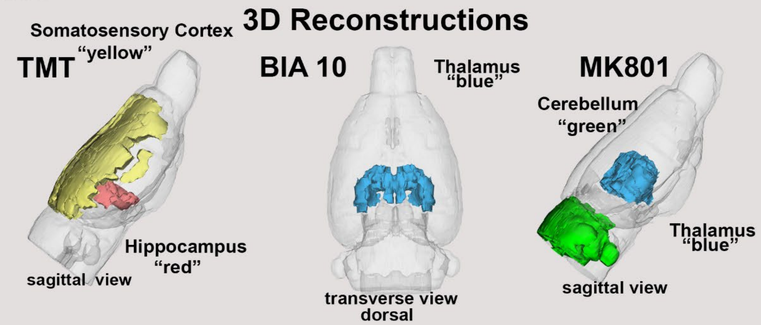

C. MK801

MK801	Vehicle			MK801		
Brain Area	Ave	SD		Ave	SD	P val
lateral amygdala	2.12	0.27	<	2.76	0.31	0.009
5th cerebellar lobule	2.15	0.17	<	2.91	0.43	0.009
ectorhinal ctx	1.98	0.07	<	2.71	0.23	0.009
inferior colliculus	2.22	0.16	<	2.93	0.50	0.009
trapezoid body	2.24	0.26	<	3.24	0.66	0.009
root of trigeminal nerve	2.57	0.28	<	3.23	0.53	0.016
4th cerebellar lobule	2.10	0.19	<	2.86	0.52	0.016
6th cerebellar lobule	1.89	0.26	<	2.62	0.38	0.016
entorhinal ctx	2.36	0.20	<	2.90	0.32	0.016
parvicellular reticular n.	2.36	0.20	<	3.22	0.65	0.016
raphe magnus	2.17	0.18	<	3.19	0.70	0.016
cochlear n.	2.23	0.27	<	3.01	0.50	0.016
subiculum dorsal	2.22	0.13	<	2.77	0.48	0.021
basal amygdala	2.06	0.18	<	2.54	0.32	0.028
dentate gyrus dorsal	2.09	0.12	<	2.56	0.41	0.028
caudal piriform ctx	2.08	0.11	<	2.56	0.25	0.028
perirhinal ctx	2.11	0.25	<	2.62	0.33	0.028
3rd cerebellar lobule	2.20	0.27	<	2.98	0.56	0.028
7th cerebellar lobule	1.88	0.21	<	2.60	0.56	0.028
8th cerebellar lobule	1.90	0.28	<	2.69	0.50	0.028
9th cerebellar lobule	2.04	0.34	<	2.91	0.57	0.028
anterior pretectal n.	1.93	0.20	<	2.53	0.48	0.028
CA1 dorsal	2.04	0.08	<	2.52	0.41	0.028
gigantocellular reticular n.	2.42	0.23	<	3.29	0.67	0.028
lateral dorsal thalamus	2.03	0.23	<	2.44	0.37	0.028
medial cerebellar n. fastigial	2.51	0.40	<	3.32	0.52	0.028
periaqueductal gray	2.24	0.16	<	2.81	0.55	0.028
pontine nuclei	2.41	0.32	<	3.12	0.60	0.028
periolivary n.	2.67	0.33	<	3.57	0.73	0.028
parietal ctx	2.00	0.17	<	2.51	0.42	0.028
primary SS ctx trunk	1.98	0.16	<	2.48	0.39	0.028
substantia innominata	2.20	0.22	<	2.65	0.37	0.028
superior colliculus	2.03	0.15	<	2.72	0.53	0.028
visual 1 ctx	2.11	0.26	<	2.66	0.35	0.028
vestibular n.	2.38	0.28	<	3.27	0.78	0.028
ventral posteriolateral thalamus	1.93	0.22	<	2.36	0.31	0.028
CA3 dorsal	2.07	0.19	<	2.53	0.41	0.036
parabrachial n.	2.12	0.28	<	2.89	0.69	0.036
zona incerta	1.96	0.23	<	2.43	0.37	0.036
paraflocculus cerebellum	2.11	0.35	<	2.70	0.33	0.047
subthalamus	2.12	0.26	<	2.64	0.45	0.047
visual 2 ctx	1.94	0.13	<	2.56	0.43	0.047
ventral posteriolmedial thalamus	1.91	0.25	<	2.38	0.39	0.047
2nd cerebellar lobule	2.32	0.18	<	2.98	0.57	0.047
anterior thalamus	1.97	0.29	<	2.50	0.47	0.047
auditory ctx	2.02	0.20	<	2.49	0.41	0.047
anterior cingulate ctx	2.04	0.15	<	2.47	0.33	0.047
crus 1 of ansiform lobule	1.85	0.23	<	2.46	0.45	0.047
dorsal lateral striatum	1.84	0.23	<	2.19	0.26	0.047
inferior olivary complex	2.69	0.28	<	3.46	0.54	0.047
lateral geniculate	1.95	0.20	<	2.43	0.43	0.047
lemniscal n.	2.26	0.40	<	2.92	0.59	0.047
medial amygdaloid n.	2.68	0.17	<	3.11	0.27	0.047
paraventricular nuclus	2.41	0.26	<	2.99	0.48	0.047
parafascicular thalamus	1.92	0.26	<	2.43	0.47	0.047
paramedian lobule	2.17	0.53	<	2.73	0.43	0.047
pontine reticular n. caudal	2.14	0.21	<	2.94	0.79	0.047
posterior thalamus	1.89	0.24	<	2.40	0.43	0.047
principal sensory n. trigeminal	2.18	0.28	<	3.02	0.71	0.047
retrosplenial caudal ctx	2.34	0.26	<	3.02	0.47	0.047
simple lobule cerebellum	1.91	0.20	<	2.69	0.54	0.047
tenia tecta ctx	2.64	0.46	<	3.34	0.45	0.047
ventral anterior thalamus	1.87	0.26	<	2.39	0.39	0.047
ventrolateral thalamus	1.88	0.25	<	2.38	0.37	0.047
ventromedial thalamus	1.88	0.28	<	2.33	0.35	0.047

Shown above in Tables A., B. and C. are brain areas with significantly different measures of ADC 3 days following TMT exposure. The brain areas are ranked in order of their significance (P-val) and effect size (omega square). Shown are the average (Ave)and standard deviation (SD) for the five rats. Note that all brain areas following TMT have ADC values lower than normal a possible sign of cytotoxic edema. ADC values for BIA 10-2474 and MK-801 are greater than the vehicle, a sign of vasogenic edema. The localization of the significantly affected areas listed in the tables are presented in the 2D heat maps and 3D reconstructions.

Acknowledgement: We thank Ekam Imaging for supporting these studies.

EKAM